KTH Electrical Engineering

MEMS tunable polarization rotator for optical communication

Sandipan Das

Stockholm, February 10, 2016

Contents

Chapter 1

Introduction

Communication and collected thinking is the key to the development and continuous evolution of human civilization which is driven by data - "The new oil of this digital era". With the advent of Internet of Things (IoT), it has been estimated that by 2020 there will be 26 billion connected devices [1] and all that can be connected will be connected. Today only about 40 percent [2] of the world's population use the Internet and the amount of data produced per minute through different social media platform like Facebook, Youtube, Twitter, Flickr, Instagram, Linkedin, Blogger, Whatsapp etc. is already growing exponentially.

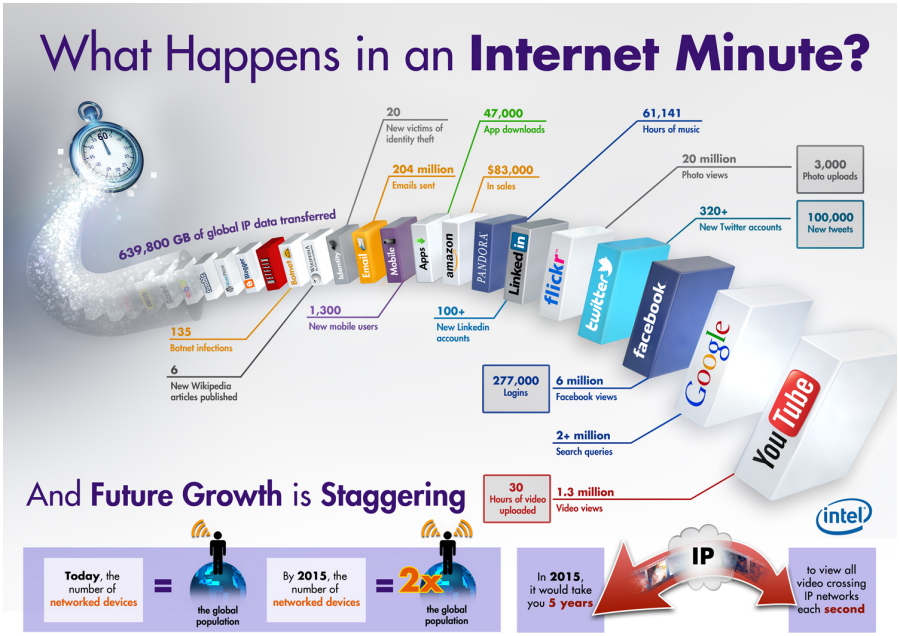

Figure 1.1: What happens on internet per minute [3]

Eventually, with the inclusion of world's population into the cyberspace world this data growth will be more than ever.

Edit this picture

Also, with the advent of mobile communications, there has been a huge surge in the voice as well as data traffic all over the world. It has been estimated in Ericsson's mobility

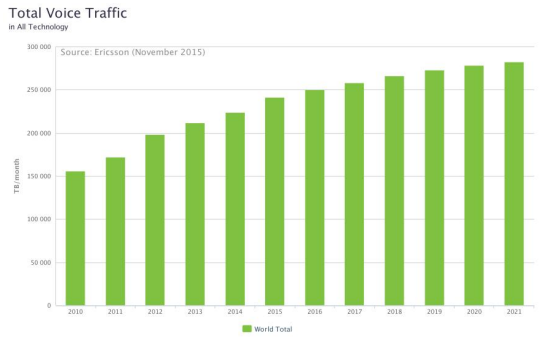

(a) Voice data traffic forecast all over the world

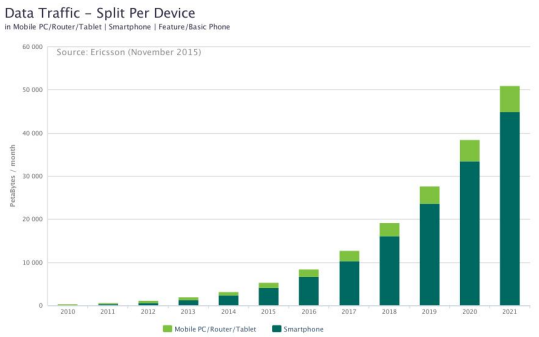

(b) Data traffic forecast for different devices

Figure 1.2: Voice and data traffic growth forecast by 2020 as per Ericsson, generated using [5]

report [4] that 70 percent of world's population will use smart-phones by 2020 and 90 percent of the world's population over 6 years old will have a mobile phone by 2020.

Currently, the telecommunications industry is moving towards IP Multimedia Subsystem (IMS) core networks which is a transition towards full IP based networks. So how is this humongous traffic managed? The answer is the optical fiber, which serves as the backbone of all the communication systems. The performance of optical fiber network is unprecedented and it is this backbone which gives us an unfathomable user experience. The current internet architecture has already pushed the optical fiber to the network edges and the trend is to push it as closer to the processor as possible. This has already opened up a new area of "Siliconizing photonics" based on the decades of research obtained from microelectronics industry. The electronics industry have pushed the boundaries of the processing speed of Integrated circuit(s) (IC) after the invention of semiconductors and are currently at the edge where Moore's Law is at its upper limit. Although, with the current technology we have a decent processing power but what about the interconnects between the IC. Transmission of signals through copper interconnects would definitely slow things down. Think of a data center processing peta-bytes of data per minute, where interconnects between processors can add up to a significant delay. These losses can be overcome by adding optical interconnects using the current technology which can also operate at low power and better efficiency catering to the needs of the environment.

1.1 Motivation

The movement of data in a computer is almost the equivalent of movement of traffic in a city, where data flows fast in the congested microprocessor but is delayed in the interconnects. Intel processor speed and bus speed comparison [6] shows that although we have achieved good processing speed, the interconnects always find difficulty in catching up with the processing speed. Obviously, the closer engineers can bring the

optical superhighway to the microprocessor, the fewer copper bottlenecks can occur. Until recently, exponential increases in the speed, efficiency, and processing power of conventional electronic devices were achieved largely through the downscaling and clustering of components on a chip. However, this trend toward miniaturization has yielded unwanted effects in the form of significant increases in noise, power consumption, signal propagation delay and aggravates already to serious thermal management problems. Alternatively, the wires can be made fatter, but then you'll run out of space and the packing density will be inefficient. As a result, traditional microelectronics will soon fall short of meeting market needs, inhibited by the thermal and bandwidth bottlenecks inherent in copper wiring. Photons don't suffer from these limitations; their biggest problems are absorption and attenuation, neither of which is an issue over the distances inside a computer, or even across a room. Today Silicon Photonics [7] Technology is a new approach to make optical devices out of silicon and use light (photons) to move huge amounts of data at very high speeds with extremely low power over a thin optical fiber rather than using electrical signals over a copper wire. Since, already enough capital investments has been done on perfecting the current fabrication technology and infrastructure, engineers are working on creating monolithic design of integrated circuits which use light in place of electric signals. Organizations are trying to bridge this gap by creating highly integrated photonic and electronic components that combine the functionality of conventional Complementary metal-oxide semiconductor (CMOS) circuits with the significantly enhanced system performance of photonic solutions. By allowing for the seamless integration of optical and electronic components on silicon-based substrates, this technology holds the key to fulfilling market needs for higher bandwidth and processing speed at lower power and cost.

Silicon Photonics is an emerging market and researchers are actively working on creating monolithic IC design with optical components to cope up with the future demands [8]. Researchers are coming up with new avenues indicating that fiber information capacity can be notably increased over previous estimates [9] which can double fiber optic capacity. The silicon photonics market is estimated to grow to 700 million USD by 2024 [10] with a Compound annual growth rate (CAGR) of 38 percent. Photonic devices made on Silicon on Insulator (SOI) platform is compatible with CMOS electrical circuits since they are based on same material. It is also promising in developing on-chip integration for telecommunications applications and servers in data centers [11]. Various kinds of silicon photonic devices like switches [12, 13, 14], modulators [15, 16], photodetectors [17, 18], delay lines [19, 20], sensors [21, 22, 23] etc. have been reported till date. All these things have corroborated interest into silicon photonics which are based on SOI platform.

However, these photonic devices based on SOI waveguides are sensitive to polarization due to large structural birefringence, which might induce Polarization dependent loss (PDL), Polarization mode dispersion (PMD), and Polarization dependent wavelength characteristics (PDλ) limiting their usability. To overcome these challenges Polarization rotator (PR) are engineered on SOI for Optoelectronic integrated circuit (OEIC) and various designs have already been demonstrated [24, 25, 26, 27, 28, 29, 30] which will be discussed in later sections. The main principle of these proposed solutions are based on

varying Refractive index (RI) by introducing asymmetry in the waveguide structure which is not tunable. Also, in some cases the designs [31], if used in commercial applications for miniature interconnects, would incur inefficient packing density since too much space is required to achieve high and robust tuning. Apart from that there might also be thermo-optic induction problem which might change phase of the wave in other waveguides in high compact density environment as silicon is highly susceptible to thermal changes [32]. Also, Tunable polarization rotator (TPR) have been reported which works on the principle of Berry's phase, a quantum-mechanical phenomenon of purely topological origin [33]. But, since the design is based on out of plane waveguides it might be difficult to achieve efficient mass production without a complex manufacturing process. The general goal of the thesis work to realize efficient TPR using Microelectromechanical systems (MEMS) to achieve improvement over the current available research solutions, to cater needs of the future industry.

1.2 Objectives

The current situation landscape in Silicon Photonics is quite exciting and a number of problems are there in the industry to realize a final optimal and robust prototype. The main objective of this thesis work is to design and fabricate low power TPR which can primarily mitigate the drawbacks discussed earlier. To tune at sufficient low power, MEMS. The waveguides will be build upon current Silicon fabrication technology which will be characterized using an automated measurement setup to minimize coupling loss using grating couplers. In this thesis following objectives will be addressed:

- ☐ How to design a MEMS tunable polarization rotator?
- ☐ How to simulate the design using MEMS techniques like Comsol, CST etc.?
- ☐ How to effectively characterize the system with the measurements available?
- ☐ By how much can the power consumption be reduced in comparison to current state of the art?
- ☐ What is the polarization extinction range/ratio (PER) that can be achieved through redesign?
- ☐ What packing density can be achieved through this design in comparison to the available solution for OEIC?
- ☐ How easily can the design be fabricated?
- ☐ Efficiency of the fabricated device?

1.3 MEMS and silicon photonics

MEMS are micrometre-sized sensors and actuators that are used in many devices in our everyday life (eg. Gyrometer and accelerometer in our smartphones). Using the same fabrication technology, one can fabricate on-chip optical circuits, which drastically improve the performance of telecommunication systems. However, both MEMS and silicon waveguides have been independently developed. This project aims to bring together both fields to try out new ideas to enable new applications and to improve existing ones.

1.4 Importance of these systems

Silicon photonics is on the verge of creating a newer technology trend. It is on the brink of creating a technological revolution where semiconductor industry stood back 60 years from now just before the discovery of transistors. If this technology is developed successfully it can keep up with the tremendous data processing power needed by the current networking servers to deliver services. Since use of optics can also increase the bandwidth in a many-fold manner it can cater the needs of data rate needed by the futuristic networks. Also, as the vision is to move everything closer to the chip this technology can deliver IC which can be easily fit into futuristic devices. Using MEMS for the tuning will ensure high resolution at very low standing power. This is also important because light transmitted to an optical circuit will typically come from an optical fibre, and optical fibres emit light with random polarization. Theses systems can expand the boundary of optical networks and bring it closer to the end devices by transgressing the network edges where optical fibers are currently located.

1.5 Outline of this thesis

The outline of the thesis is as follows: Background, motivation and the research questions being addressed, is discussed in Chapter 1. In Chapter 2, the current state of art for the available solution is discussed along with the background literature required. Here, also the working principle of the current available design are explained along with the areas which can be improved. Chapter 3 discusses about the design of the final system and the results obtained about the simulation setup. In Chapter 4, documentation about the fabricated design is provided along with currently available standard fabrication technologies. Results and characterization are an important part of the work, which is discussed in Chapter 5. Finally, Chapter 6 and 7 discusses about the conclusion and future work possibilities respectively along with the known limitations of the system if any.

Chapter 2
2 State of the art

The most interesting aspect of fabricating optical waveguides from silicon is based on low primary cost of material, the mature and evolved manufacturing techniques owing to decades of research and the potential to develop monolithic IC using the same substrate.

2.1 Theoretical background of SOI waveguide

Although silicon is the optimal material for electronics, only recently silicon is being considered as a practical option for OEIC solutions. Silicon has many properties conducive to fiber optics. The band gap of silicon (∼1.1 eV) is such that the material is transparent to wavelengths commonly used for optical transport (∼1.3 µm-1.6 µm). One can use standard CMOS processing techniques to sculpt optical waveguides onto the silicon surface. Similar to an optical fiber, these optical waveguides can be used to confine and direct light as it passes through the silicon [34]. Due to the wavelengths typically used for optical transport and silicon's high index of refraction, the feature sizes needed for processing these silicon waveguides are on the order of 0.5 µm-1 µm. The lithography requirements needed to process waveguides with these sizes exist today. If we push forward to leading-edge research currently under way in the area of Photonic band-gap (PBG) devices, today's state-of-the-art 90 nm fabrication facilities should meet the technical requirements needed for processing PBG devices. What this says is that we may already have all or most of the processing technologies needed to produce silicon-based photonic devices for the next decade. In addition, the same carriers used for the basic functionality of the transistor (i.e. electrons and holes) can be used to modulate the phase of light passing through silicon waveguides and thus produce 'active' rather than passive photonic devices. Finally, if all this remains CMOS-compatible, it could be possible to process transistors alongside photonic devices, the combination of which could bring new levels of performance, functionality, power and size reduction, all at a lower cost.

2.1.1 Maxwell's equations

Light is high frequency Electromagnetic (EM) phenomenon having wave-particle duality. Visible light, ultraviolet light, and infrared light are all electromagnetic waves of differing frequency. James Clerk Maxwell discovered that he could combine four simple equations,

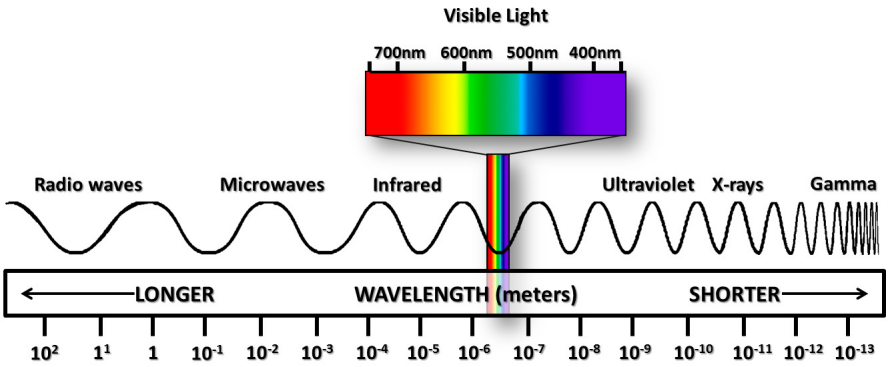

Figure 2.1: The EM wave spectrum

which had been previously discovered, along with a slight modification to describe self-propagating waves of oscillating electric and magnetic fields [35]. The understanding of propagating of light waves using Maxwell's equations in a dielectric medium, is the key to the construction of silicon waveguides. Maxwell's equations relate the electric field E (V/m), magnetic field H (A/m), charge density ρ (C/m3), and current density J (A/cm2).

- **Maxwell's first equation (Gauss' Law)**: The net electric flux through any closed surface is equal to $\frac{1}{\epsilon_m}$ times the charge density within that closed surface.

$$\nabla.E = \frac{\rho}{\epsilon_m} \tag{2.1}$$

  where ϵ_m the permittivity of the medium, and del operator, ∇, is given by:

$$\nabla = \left(\frac{\partial i}{\partial x}, \frac{\partial j}{\partial y}, \frac{\partial k}{\partial z}\right) \tag{2.2}$$

  where i, j and k are unit vectors in the x, y and z directions respectively.

- **Maxwell's second equation (Gauss' Law for magnetic field)**: The net magnetic flux through a closed surface is always zero since magnetic monopoles do not exist.

$$\nabla.H = 0 \tag{2.3}$$

- **Maxwell's third equation (Faraday's law)**: Induced electric field around a closed path is equal to the negative of the time rate of change of magnetic flux enclosed by the path.

$$\nabla \times E = -\mu_m \frac{\partial H}{\partial t} \tag{2.4}$$

  where μ_m is the permeability of the medium.

- **Maxwell's fourth equation (Modification of Ampere's law)**: The fourth equation states that magnetic fields can be generated in two ways: by electric current (this was the original "Ampere's law") and by changing electric fields (this was "Maxwell's addition") [36].

$$\nabla \times H = J + \epsilon_m \frac{\partial E}{\partial t} \tag{2.5}$$

All these equations combine into a simple wave equation after some mathematical calculations.

$$\nabla^2 E - \mu_m \epsilon_m \frac{\partial^2 E}{\partial t^2} = \mu_m \frac{\partial J}{\partial t} + \frac{\nabla \rho}{\epsilon_m} \tag{2.6}$$

using the curl of curl identity operation given by:

$$\nabla^2 E = \nabla(\nabla.E) - \nabla \times (\nabla \times E) \tag{2.7}$$

A general solution to the equation 2.6 in free space, in absence of charge gives the following solution:

$$\overrightarrow{E}(z,t) = E_0(x,y)e^{i(k_0 z \pm \omega t)} \tag{2.8}$$

where z is direction of propagation of wave in Cartesian coordinates , phase $(\phi) = (k_0 z \pm \omega t)$ and wave vector propagation constant $(k_0) = \dfrac{\partial \phi}{\partial t} = \dfrac{2\pi}{\lambda}$, in the direction of propagation of the wave. It is worth mentioning that propagation constant in medium varies according to n, the effective RI of the medium and is given by:

$$k = nk_0 \tag{2.9}$$

Similar calculations for the magnetic field, H in free space yields,

$$\overrightarrow{H}(z,t) = H_0(x,y)e^{i(k_0 z \pm \omega t)} \tag{2.10}$$

2.1.2 Eigenvalue and wave modes

In general, the electric field in the wave equation in 2.8 can be written in its constituent parts in Cartesian coordinates as:

$$\overrightarrow{E} = E_x i + E_y j + E_j k \tag{2.11}$$

If the wave propagates towards z-direction through any waveguide medium and is a Tansverse Electromagnetic (TEM) wave front then we will have a constant electric field vector in the z-direction. In this case there will be different solutions for the propagation constant, k in x and y directions. Now for each solution we can also get certain discrete angles at which the electric field can travel through the medium, which infers that light can propagate only at certain discrete angles through any dielectric medium. Each allowed solution is referred to as the *mode of propagation* and are basically the different eigenvalues of the propagation vector. In the Fig. 2.2 the electric field and magnetic

field propagate in directions perpendicular to each other. Moreover, the direction of propagation is also transverse to the EM field. Hence it is called TEM wave.

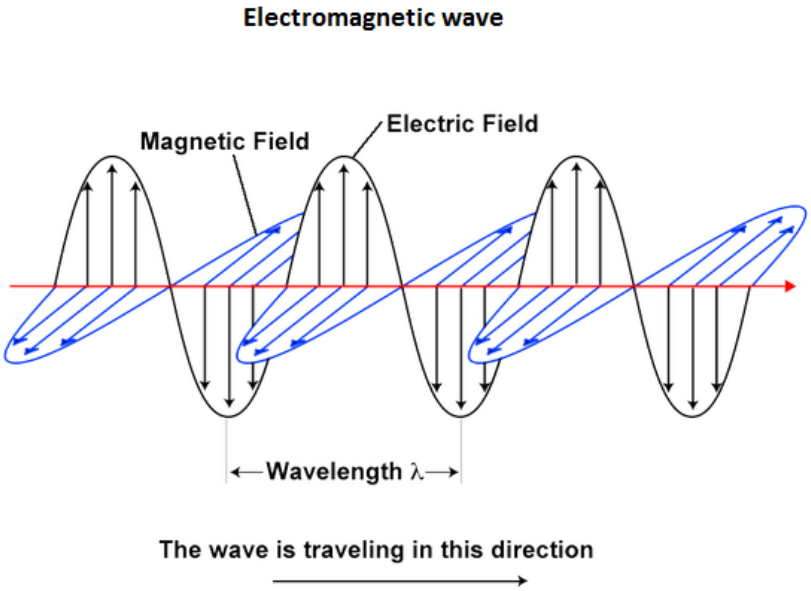

Figure 2.2: Propagation of EM wave

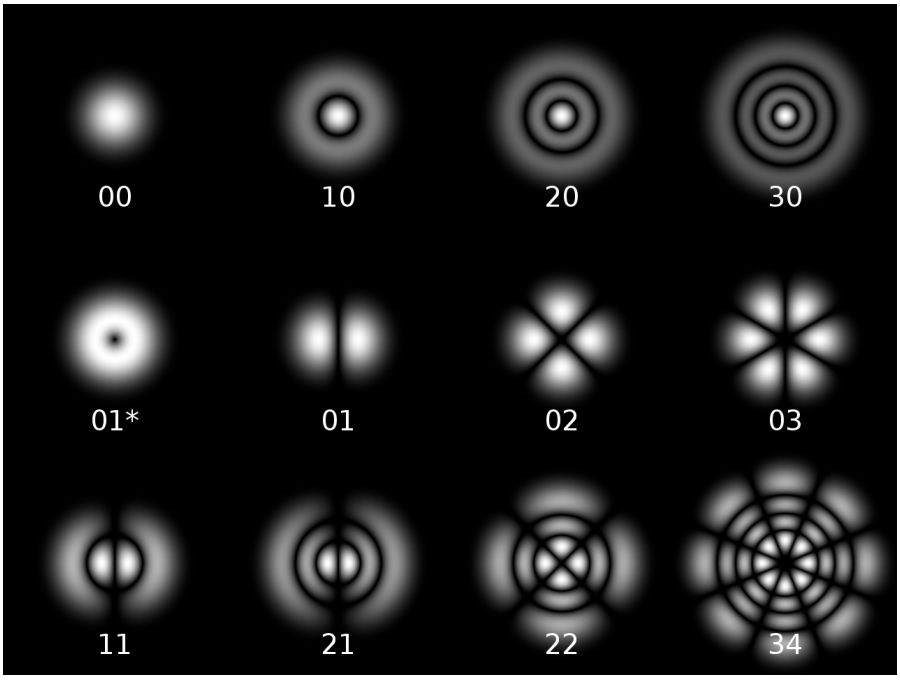

Figure 2.3: Propagation modes in optical fiber

The eigenvalues provide the different acceptance angles at which light can be inserted into the waveguide resulting in different modes in the waveguide. Depending on various angles of incidence on the waveguide and the dimensions of the waveguide, various modes can be found which are basically the different eigenvalues of the wave solution 2.8 and 2.10. For example, when light travels through optical fibers different modes can be visualized as follows in Fig. 2.3.

May be update the picture using CST

2.1.3 Optical polarization and transverse modes

Generally light in randomly polarized. Any kind of randomness is inefficient for data transmission. Optical fibers generally operate at 1550 nm in fundamental Tansverse Electric (TE) or Tansverse Magnetic (TM) mode. The ultimate goal of the on chip fabricated waveguide is to integrate with the currently deployed optical fiber network in a seamless manner. Hence, the waveguides must cater polarization into its design. *Polarization* is the direction of the electric field associated with the propagating wave.

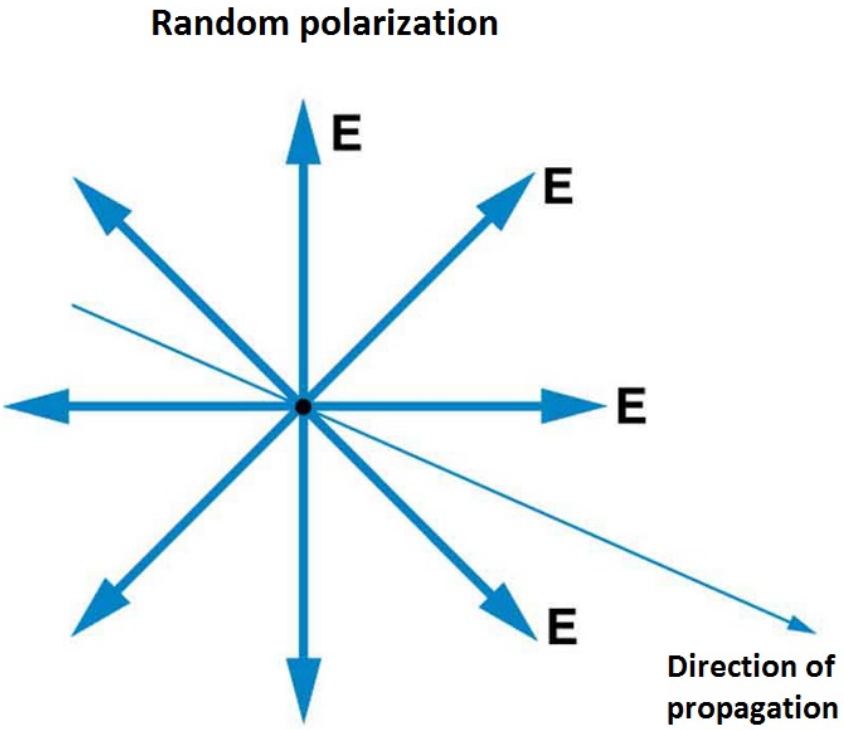

Figure 2.4: Random polarization of light

However, the associated magnetic field is not always considered in the quantum domain for wave propagating at 1550 nm. In the example in Fig. 2.2 the wave is polarized since the electric field and magnetic field exist in one direction only. In a semiconductor optical waveguide light propagates in plane polarized modes and the plane in which light is polarized is either vertical or horizontal to the waveguide surface as shown in Fig. 2.5.

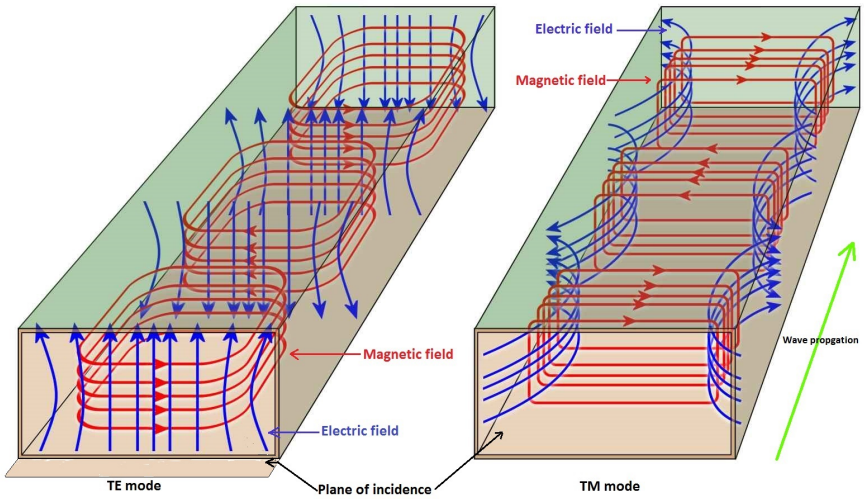

Figure 2.5: TE and TM modes in a waveguide

2.1.3.1 TE mode

TE mode is the fundamental mode in which electric field is perpendicular to the plane of incidence of light. As depicted in Fig. 2.5 it can be visualized that electric field lines shown by the blue lines are perpendicular to the plane of incidence in TE mode. The plane of incidence is the plane in which optical waves strike the surface of the waveguide.

2.1.3.2 TM mode

TM mode is the fundamental mode in which magnetic field is perpendicular to the plane of incidence of light. As shown in Fig. 2.5 it can be visualized that magnetic field shown by the red lines are perpendicular to the plane of incidence in TM mode.

2.1.4 Optical waveguides

Waveguide is the essential element of every photonic circuit which can be characterized by the number of dimensions in which light is confined inside it [37]. A planar waveguide confines light in 1-D which is simple for understanding of the wave propagation using Maxwell's equations. However, for practical applications 2-D confinement is necessary and that is why channel waveguides are used. Structures like photonic crystals even have 3-D confinement properties.

2.1.4.1 Planar waveguides

A simple planar waveguide consists of a high-indexed medium with height h surrounded by lower indexed materials on the top and bottom sides. The RI of the film, n_f (generally made from Si) is greater than the RI of the materials on the other sides. The RI of

the substrate in lower cladding is n_s, (generally made from SiO_2) whereas, RI of the substrate in upper cladding is n_c (generally which is air).

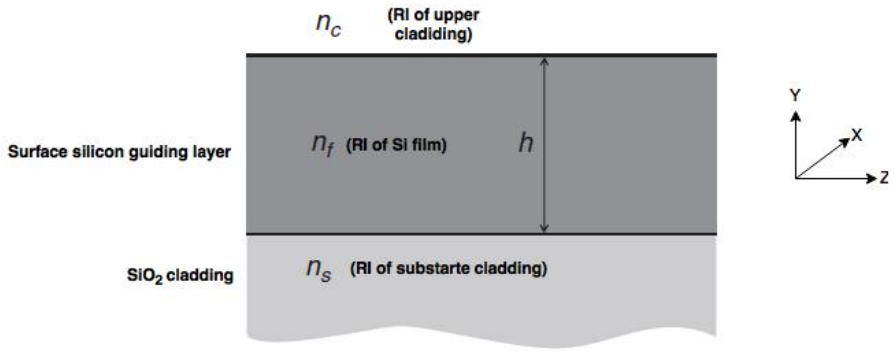

Figure 2.6: A typical planar waveguide where the film is infinite in XZ-plane

For planar waveguides the wave equation for electric field 2.8 and magnetic field can be rewritten as 2.10 follows:

$$\begin{cases} \overrightarrow{E}(z,t) = E_x(y)e^{i(k_0 z \pm \omega t)} \\ \overrightarrow{H}(z,t) = H_x(y)e^{i(k_0 z \pm \omega t)} \end{cases} \tag{2.12}$$

since in X-direction the film is infinite. After using the homogeneous wave equations for a planar waveguide the following TE and TM mode equations can be deduced:

$$\begin{cases} \nabla^2 E_x(y) + (k_0^2 n(y)^2 - k^2)E_x(y) = 0 \\ \nabla^2 H_x(y) + (k_0^2 n(y)^2 - k^2)H_x(y) = 0 \end{cases} \tag{2.13}$$

where RI depends only on a single Cartesian coordinate $n = n(y)$. These equations can be solved using the various boundary conditions of the waveguides which help in deducing the nature of propagation of the wave in TE and TM mode. Different kinds of numerical methods like Finite element modeling (FEM), Finite difference time domain (FDTD), Beam propagation method (BPM) have been developed to decipher the nature of light propagation in waveguides.

2.1.4.2 Channel waveguides

As mentioned earlier channel waveguides provide confinement in 2-D which helps in depicting more practical waveguides. The three main types of channel waveguides are rib, strip and buried waveguides. As depicted in 2.7a, 2.7b, 2.7c the different conceptual structures of the waveguides can be envisaged. While the rib and strip waveguides are designed using etching technique, the buried waveguide mostly relies on diffusion and epitaxial growth technique for its fabrication.

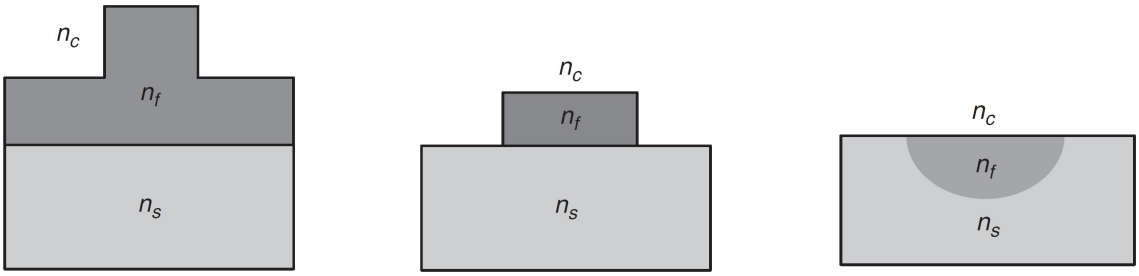

(a) Rib waveguide (b) Strip waveguide (c) Buried waveguide

Figure 2.7: Different kinds of design for channel waveguides

- **Design rules of rib waveguides:** While designing these waveguides each of these have specific design rules for optimum performance and low-loss coupling, which has been standardized after years of research [37]. The Single-mode condition (SMC) for *rib waveguides* is as follows:

$$\frac{W}{H} \leq 0.3 + \frac{r}{\sqrt{1-r^2}}, \quad \text{for } (0.5 \leq r < 1) \tag{2.14}$$

where W=waveguide width, H=rib height, r is ratio of slab height to overall rib height.

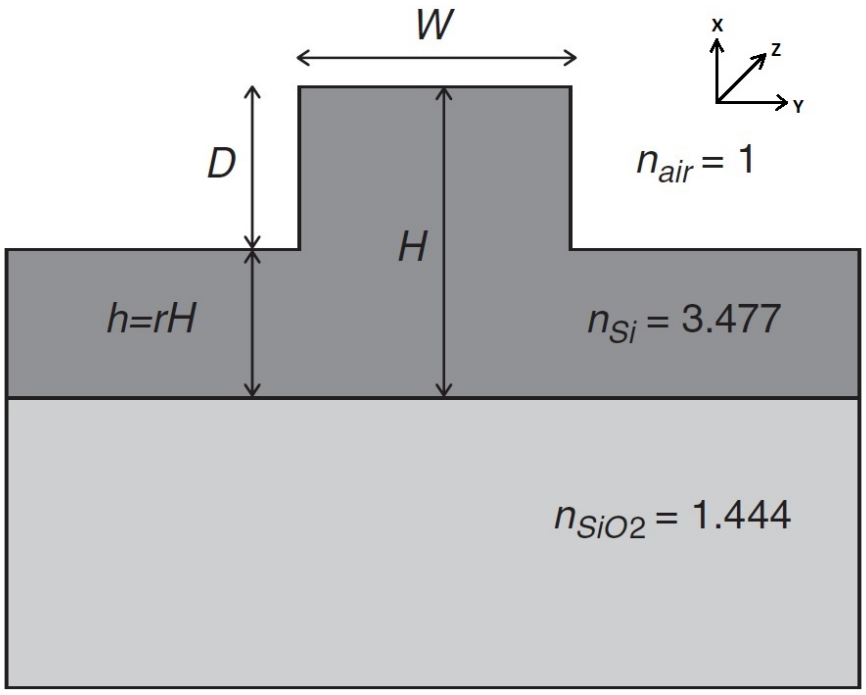

Figure 2.8: Rib waveguide design rules

The main requirements of the waveguide to cater the propagation of waves is that the dimension of the waveguide has to be more than the wavelength of the

propagating wave. However, depending on the required structure the design rules may change which can be found using simulation.

- **Design rules of strip waveguides:** In mode confinement of light in optical waveguides the effective mode RI is important. Strip waveguides offer more high RI contrast in comparison to Rib waveguides. This can help in realization of ultra-dense photonic circuits because of high effective mode confinement. This can also achieve small bends which can improve the characterization of different monolithic optical circuits. In general a mix of rib and strip waveguides are used to achieve the desired circuitry, since sometimes the side walls cannot be etched in a perfectly smooth way causing greater evanescent fields from the waveguides introducing unnecessary coupling and losses. Using simulation for the desired scenario the robust values of the dimensions can be achieved.

2.1.5 Confinement factor

Often it is necessary to know the confined power inside the core of the waveguide which helps in figuring out the waveguide mode. The confinement is also a measure of the proportion of the power in a given mode that lies within the core [37].

$$\text{Confinement factor } = \frac{\int_{-H/2}^{H/2} E_x^2(y)\,dy}{\int_{-\infty}^{\infty} E_x^2(y)\,dy} \tag{2.15}$$

Confinement factor is an important measure which is function of various factors like polarization, RI difference between the core and cladding, mode number etc.

2.1.6 Jones calculus

Polarized light can be represented using Jones calculus. Polarized light is represented using *Jones vector* and linear optical elements are represented by *Jones matrices*. When light crosses an optical element the resulting polarization of the emerging light is found by taking the product of the Jones matrix of the optical element and the Jones vector of the incident light. *Jones calculus* is only applicable to light that is **already fully polarized** [38].

2.1.6.1 Jones vector

The Jones vector describes the polarization of light in free space or another homogeneous isotropic non-attenuating medium, where the light can be properly described as transverse waves [38]. The Jones vector is a complex vector that is a mathematical representation of a real wave. A typical representation of the electric field for the optical wave described in 2.8 can be as follows:

$$E = \begin{pmatrix} E_x(t) \\ E_y(t) \\ 0 \end{pmatrix} = \begin{pmatrix} E_x e^{i(kz-\omega t+\phi_x)} \\ E_y e^{i(kz-wt+\phi_y)} \\ 0 \end{pmatrix} = \begin{pmatrix} E_x e^{i\phi_x} \\ E_y e^{i\phi_y} \\ 0 \end{pmatrix} e^{i(kz-\omega t)} \tag{2.16}$$

where ϕ_x and ϕ_y indicate the phasor notation. The Jones vector of the plane wave is described by:

$$\begin{pmatrix} E_x e^{i\phi_x} \\ E_y e^{i\phi_y} \end{pmatrix} \tag{2.17}$$

and the intensity of the optical, I wave can be written as,

$$I = |E_x|^2 + |E_y|^2 \tag{2.18}$$

Generally, when considering Jones vector a wave of unit intensity is required for the consideration polarization, so Jones vector is noted using an unit vector where,

$$E\overline{E} = 1 \tag{2.19}$$

where $\overline{E}$ is the complex conjugate of E. In general the Jones representation of a normalized elliptically polarized beam with azimuth θ and elliptical angle ϵ is given by,

$$e^{i\phi} \begin{pmatrix} \cos\theta\cos\epsilon - j\sin\theta\sin\epsilon \\ \sin\theta\cos\epsilon - j\cos\theta\sin\epsilon \end{pmatrix} \tag{2.20}$$

where $e^{i\phi}$ is an arbitrary phase vector and $\phi = \phi_x - \phi_y$. So, for example a linear polarization of TE mode can be represented as,

$$\begin{pmatrix} 1 \\ 0 \end{pmatrix} \tag{2.21}$$

since, $\theta = 0$ and $\epsilon = 0$.

2.1.6.2 Jones matrix

Jones matrix are the formal representation of the various optical elements such as lenses, beam splitters, mirrors, phase retarders, polarizers at arbitrary angles that can modify polarization. They generally operate on Jones vector and helps in comprehend situations which light encounters multiple polarization elements in sequence. In these situations the products of the Jones matrices can be used to represent the transfer matrix. This situation can be represented using,

$$[E_{output}] = J_{system}[E_{input}] \tag{2.22}$$

where E_input is the input field into the optical system and E_output is the generated output field represented using Jones vector. The matrix J_system is the Jones matrix of the optical system comprising of a series of polarization devices. If there are N devices in the system then the final transfer matrix comes out as,

$$J_{system} = J_N J_{N-1} \ldots\ldots J_2 J_1 \tag{2.23}$$

where J_N is the Jones matrix for n^{th} polarizing optical element.

2.1.7 Jones matrix for polarizing optical systems

To construct optical waveguides for polarization rotation it is imperative to deal with the basic principles of standard available optical systems. Here, the fundamental principles of polarizer and wave plates are interpreted using Jones calculus.

2.1.7.1 Polarizer

Polarizers have an index of refraction which depends on orientation electric field propagation. If any optical system has a transmission axis and an absorption axis for electric fields, then lights will be passed along he transmission axis and absorbed along the other axis. So, the Jones matrix of a polarizer making an angle θ with the X-axis will come out as,

$$\begin{pmatrix} \cos^2\theta & \sin\theta\cos\theta \\ \sin\theta\cos\theta & \sin^2\theta \end{pmatrix} \tag{2.24}$$

2.1.7.2 Wave plate

Wave plates are phase retarders which are made of birefringent crystals. Wave plates can be conceptualized as two polarizers kept apart at certain distance d, such that their polarization axes are apart orthogonally (90^0). The phase difference as light passes through this setup of thickness d is,

$$(k_{slow} - k_{fast})\, d = \frac{2\pi d}{\lambda_{vac}} (n_{slow} - n_{fast}) \tag{2.25}$$

In, general the Jones matrix for a wave plate is given by,

$$\begin{pmatrix} \cos^2\theta + \xi\sin^2\theta & \sin\theta\cos\theta - \xi\sin\theta\cos\theta \\ \sin\theta\cos\theta - \xi\sin\theta\cos\theta & \sin^2\theta + \xi\cos^2\theta \end{pmatrix} \tag{2.26}$$

where ξ is calculated based on the type of wave plate. The following equations addresses some general scenarios:

$$\begin{cases} \xi = e^{i\pi/2}, & \text{where, } (k_{slow} - k_{fast})\, d = \pi/2 + 2\pi m, \text{for quarter-wave plate} \\ \xi = e^{i\pi}, & \text{where, } (k_{slow} - k_{fast})\, d = \pi + 2\pi m, \text{for half-wave plate} \end{cases} \tag{2.27}$$

Similar concept is used in the construction of PR waveguides which will be discussed in later sections shortly.

2.1.8 Poincaré sphere and state of polarization

To view a complete representation of all the polarization ellipses generated using Jones vectors, a spherical structure with unit radius is used, which is known as Poincaré sphere. If the orientation in space of of the ellipse of polarization is determined by the azimuth, θ and ellipticity, ϵ then that point can be completely characterized by its longitude 2θ

and latitude 2ϵ. The north and south poles represent the right-handed and left-handed circular polarization respectively. In general the diametrically opposite points represent pairs of orthogonal polarization. The State of polarization (SOP) and its corresponding location in the Poincaré sphere is visualized in the Fig. 2.9. To go from one SOP to another the polarized light can be passed through various optical components which can be computed using the Jones matrix and the corresponding SOP can be depicted on the Poincaré sphere as well.

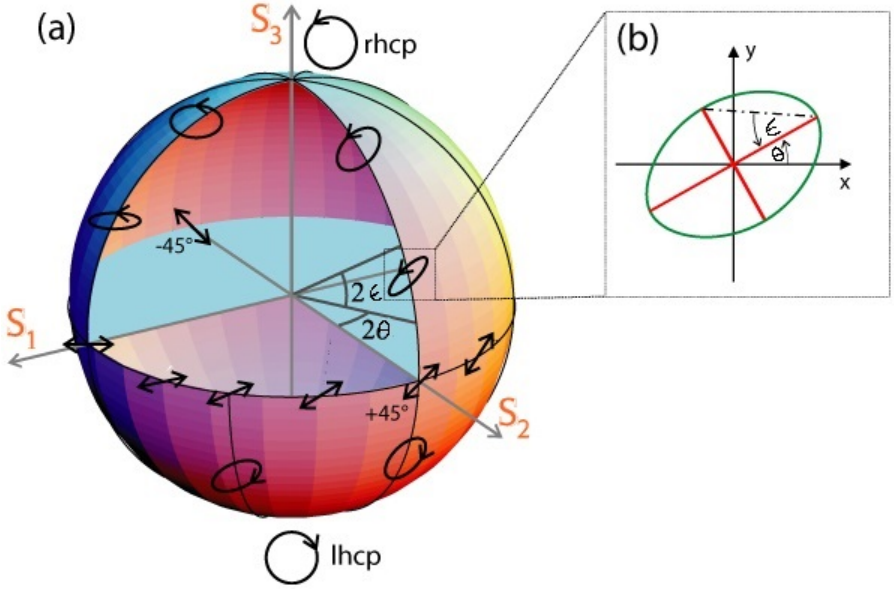

Figure 2.9: (a) Representation of the Poincaré sphere (b) Representation of the ellipse parameters [39]

The SOP of any wave is also defined using PER and polarization phase, ϕ given by the following equations:

$$\begin{aligned} PER_{TE-TM} &= 10 \log \frac{P_{TM}}{P_{TE}} \\ PER_{TM-TE} &= 10 \log \frac{P_{TE}}{P_{TM}} \\ \phi &= \phi_x - \phi_y \end{aligned} \tag{2.28}$$

For complete polarized light, the point on the Poincaré sphere must be fixed on time which requires,

$$\frac{E_x(t)}{E_y(t)} = constant \tag{2.29}$$

and,

$$\phi = \phi_x(t) - \phi_y(t) = constant \tag{2.30}$$

2.1.9 Stoke's parameter

Quasi-monochromatic waves are mathematically treated using Stokes parameters (S_0, S_1, S_2, S_3), which constitute a vector generally known as Stokes vectors. Stokes vectors are used to keep track of the partial polarization (and attenuation) of a light beam in terms of total intensity (I), degree of polarization (p) and ellipse parameters, as the light progresses through an optical system. A Stokes vector can generally be represented as,

$$\overrightarrow{S} = \begin{pmatrix} S_0 \\ S_1 \\ S_2 \\ S_3 \end{pmatrix} \tag{2.31}$$

where,

$$\begin{cases} S_0 = I \\ S_1 = I_p \cos 2\theta \cos 2\epsilon \\ S_2 = I_p \sin 2\theta \cos 2\epsilon \\ S_3 = I_p \sin 2\epsilon \end{cases} \tag{2.32}$$

Here, $I_p, 2\theta, 2\epsilon$ are the spherical coordinates of the 3-D vector of Cartesian coordinates (S_1, S_2, S_3). So, given the Stokes parameters, the spherical coordinates $(p, 2\theta, 2\epsilon)$ can be obtained and represented by a point inside the Poincaré sphere using the following:

$$\begin{cases} I = S_0 \\ p = \dfrac{\sqrt{S_1^2 + S_2^2 + S_3^2}}{S_0} \\ 2\theta = \tan^{-1} \dfrac{S_2}{S_1} \\ 2\epsilon = \tan^{-1} \dfrac{S_3}{\sqrt{S_1^2 + S_2^2}} \end{cases} \tag{2.33}$$

The prescribed notations are portrayed on the Poincaré sphere in the following Fig. 2.10.

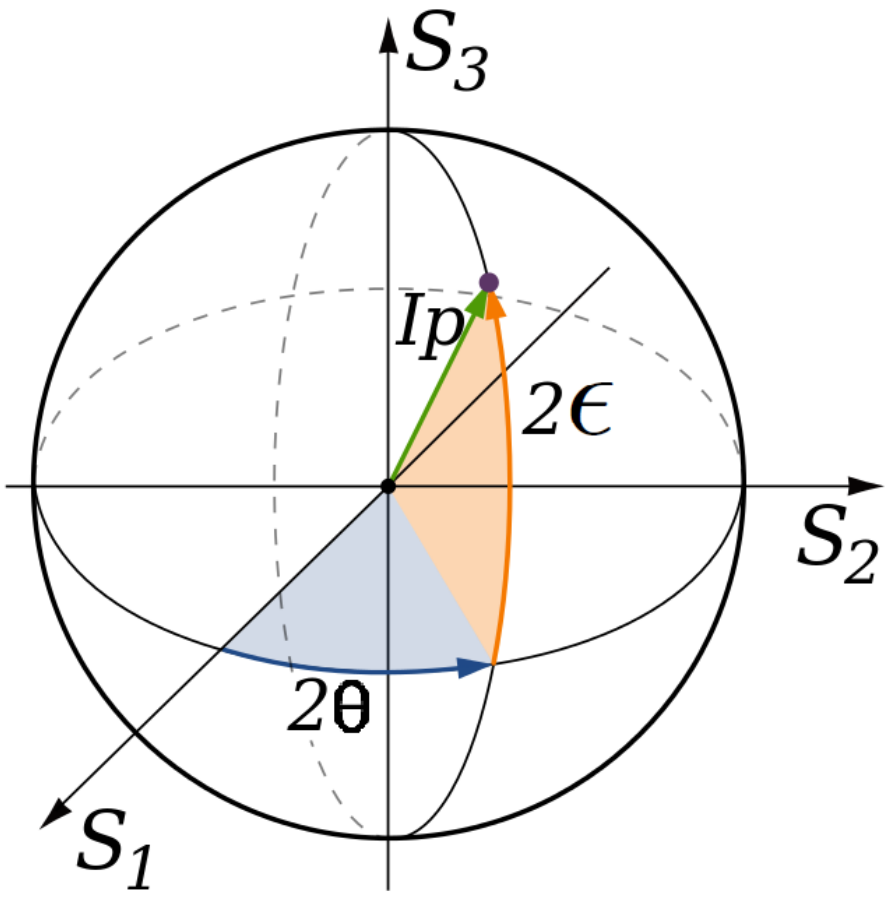

Figure 2.10: Poincaré sphere, on or beneath which the three Stokes parameters [S1, S2, S3] are plotted in Cartesian coordinates [41]

2.2 Theoretical background of MEMS

2.2.1 Overview

2.2.2 Actuation principle

2.3 Polarization rotator

2.3.1 Passive polarization rotator

2.3.2 Active polarization rotator

Chapter 3

3 Design and simulation

3.1 Approach

3.2 Designing the experiment

3.2.1 Design principle

3.2.2 Use case: Active polarization rotator

3.3 Choice of simulation

3.4 Simulation results and analysis

Chapter 4

4 Fabrication

Chapter 5

5 Results

5.1 Experimental setup for measurement

5.2 Optical coupling

5.3 Results

5.4 Analysis

Chapter 6

6 Conclusions

Chapter 7

7 Limitations and future work

7.1 Limitations

7.2 Future work

Todo list

Abbreviations

BPM Beam propagation method. 12

CAGR Compound annual growth rate. 3

CMOS Complementary metal-oxide semiconductor. 3, 6

EM Electromagnetic. 6, 7, 9

FDTD Finite difference time domain. 12

FEM Finite element modeling. 12

IC Integrated circuit(s). 2, 3, 5, 6

IMS IP Multimedia Subsystem. 2

IoT Internet of Things. 1

MEMS Microelectromechanical systems. 4, 5

OEIC Optoelectronic integrated circuit. 3, 4, 6

PBG Photonic band-gap. 6

PDλ Polarization dependent wavelength characteristics. 3

PDL Polarization dependent loss. 3

PER polarization extinction range/ratio. 4, 15

PMD Polarization mode dispersion. 3

PR Polarization rotator. 3

RI Refractive index. 4, 8, 11, 12, 14

SMC Single-mode condition. 13

SOI Silicon on Insulator. 3

SOP State of polarization. 15

TE Tansverse Electric. 10–12

TEM Tansverse Electromagnetic. 8, 9

TM Tansverse Magnetic. 10–12

TPR Tunable polarization rotator. 4

Bibliography

[1] "Gartner says the internet of things installed base will grow to 26 billion units by 2020." http://www.gartner.com/newsroom/id/2636073, 2013. [Online; accessed 26-Jan-2016].

[2] "Number of Internet Users (2015) - Internet Live Stats." http://www.internetlivestats.com/internet-users/, 2015. [Online; accessed 22-Jan-2016].

[3] "What Happens in an Internet Minute [Infographic] | Daily Infographic." http://www.dailyinfographic.com/what-happens-in-an-internet-minute-infographic, 2013. [Online; accessed 29-Jan-2016].

[4] "Ericsson Mobility Report: 70 percent of world's population using smartphones by 2020." http://www.ericsson.com/news/1925907, 2015. [Online; accessed 06-Feb-2016].

[5] "Ericsson traffic exploration infograph." http://www.ericsson.com/TET/trafficView/loadBasicEditor.ericsson, 2015. [Online; accessed 06-Feb-2016].

[6] "ARK | Your Source for Intel® Product Specifications." http://ark.intel.com/, 2015. [Online; accessed 06-Feb-2016].

[7] "Silicon photonics." https://en.wikipedia.org/wiki/Silicon_photonics/, 2015. [Online; accessed 06-Feb-2016].

[8] N. Savage, "Linking Chips With Light." http://spectrum.ieee.org/semiconductors/optoelectronics/linking-chips-with-light, 2015. [Online; accessed 06-Feb-2016].

[9] E. Temprana, E. Myslivets, B. P.-P. Kuo, L. Liu, V. Ataie, N. Alic, and S. Radic, "Overcoming Kerr-induced capacity limit in optical fiber transmission," *Science*, vol. 348, pp. 1445–1448, June 2015.

[10] "Silicon photonics market to grow at CAGR of 38% from $25m in 2013 to $700m in 2024." http://www.semiconductor-today.com/news_items/2014/JUL/YOLE_180714.shtml, 2014. [Online; accessed 06-Feb-2016].

[11] B. Jalali and S. Fathpour, "Silicon Photonics," *Journal of Lightwave Technology*, vol. 24, pp. 4600–4615, Dec. 2006.

[12] M. C. Wu, T. J. Seok, S. Han, and N. Quack, "MEMS-Enabled Scalable Silicon Photonic Switches," p. FW3B.2, 2015.

[13] D. Nikolova, S. Rumley, D. Calhoun, Q. Li, R. Hendry, P. Samadi, and K. Bergman, "Scaling silicon photonic switch fabrics for data center interconnection networks," *Optics Express*, vol. 23, p. 1159, Jan. 2015.

[14] L. Lu, L. Zhou, X. Li, and J. Chen, "Low-power 2x2 silicon electro-optic switches based on double-ring assisted Mach–Zehnder interferometers," *Optics Letters*, vol. 39, p. 1633, Mar. 2014.

[15] P. Dong, C. Xie, L. L. Buhl, Y.-K. Chen, J. H. Sinsky, and G. Raybon, "Silicon In-Phase/Quadrature Modulator With On-Chip Optical Equalizer," *Journal of Lightwave Technology*, vol. 33, pp. 1191–1196, Mar. 2015.

[16] C. Chen, C. He, D. Zhu, R. Guo, F. Zhang, and S. Pan, "Generation of a flat optical frequency comb based on a cascaded polarization modulator and phase modulator," *Optics Letters*, vol. 38, p. 3137, Aug. 2013.

[17] Y. Urino, Y. Noguchi, M. Noguchi, M. Imai, M. Yamagishi, S. Saitou, N. Hirayama, M. Takahashi, H. Takahashi, E. Saito, T. Shimizu, M. Okano, N. Hatori, M. Ishizaka, T. Yamamoto, T. Baba, T. Akagawa, S. Akiyama, T. Usuki, D. Okamoto, M. Miura, J. Fujikata, D. Shimura, H. Okayama, H. Yaegashi, T. Tsuchizawa, K. Yamada, M. Mori, T. Horikawa, T. Nakamura, and Y. Arakawa, "Demonstration of 12.5-Gbps Optical Interconnects Integrated with Lasers, Optical Splitters, Optical Modulators and Photodetectors on a Single Silicon Substrate," p. Tu.4.E.1, OSA, 2012.

[18] C.-M. Chang, J. H. Sinsky, P. Dong, G. de Valicourt, and Y.-K. Chen, "High-power dual-fed traveling wave photodetector circuits in silicon photonics," *Optics Express*, vol. 23, p. 22857, Aug. 2015.

[19] S. Garcia and I. Gasulla, "Design of heterogeneous multicore fibers as sampled true-time delay lines," *Optics Letters*, vol. 40, p. 621, Feb. 2015.

[20] M. Mattarei, A. Canciamilla, S. Grillanda, and F. Morichetti, "Variable Symbol-Rate DPSK Receiver Based on Silicon Photonics Coupled-Resonator Delay Line," *Journal of Lightwave Technology*, vol. 32, pp. 3317–3323, Oct. 2014.

[21] S. Janz, A. Densmore, D.-x. Xu, P. Waldron, J. Lapointe, G. Lopinski, T. Mischki, P. Cheben, A. Delâge, B. Lamontagne, and J. H. Schmid, "Silicon Waveguide Photonics for Biosensing Applications," p. IWA1, 2007.

[22] G. Lim, U. P. DeSilva, N. R. Quick, and A. Kar, "Laser optical gas sensor by photoexcitation effect on refractive index," *Applied Optics*, vol. 49, p. 1563, Mar. 2010.

[23] E. Ryckeboer, R. Bockstaele, M. Vanslembrouck, and R. Baets, "Glucose sensing by waveguide-based absorption spectroscopy on a silicon chip," *Biomedical Optics Express*, vol. 5, p. 1636, May 2014.

[24] A. Xie, L. Zhou, J. Chen, and X. Li, "Efficient silicon polarization rotator based on mode-hybridization in a double-stair waveguide," *Optics Express*, vol. 23, p. 3960, Feb. 2015.

[25] A. V. Velasco, M. L. Calvo, P. Cheben, A. Ortega-Moñux, J. H. Schmid, C. A. Ramos, i. M. Fernandez, J. Lapointe, M. Vachon, S. Janz, and D.-X. Xu, "Ultracompact polarization converter with a dual subwavelength trench built in a silicon-on-insulator waveguide," *Optics Letters*, vol. 37, p. 365, Feb. 2012.

[26] D. Leung, B. Rahman, and K. Grattan, "Numerical Analysis of Asymmetric Silicon Nanowire Waveguide as Compact Polarization Rotator," *IEEE Photonics Journal*, vol. 3, pp. 381–389, June 2011.

[27] J. Wang, B. Niu, Z. Sheng, A. Wu, X. Wang, S. Zou, M. Qi, and F. Gan, "Design of a SiO_2 top-cladding and compact polarization splitter-rotator based on a rib directional coupler," *Optics Express*, vol. 22, p. 4137, Feb. 2014.

[28] D. Dai and J. E. Bowers, "Novel concept for ultracompact polarization splitter-rotator based on silicon nanowires," *Optics Express*, vol. 19, p. 10940, May 2011.

[29] J. C. Wirth, J. Wang, B. Niu, Y. Xuan, L. Fan, L. Varghese, D. E. Leaird, and A. Weiner, "Efficient Silicon-on-Insulator Polarization Rotator based on Mode Evolution," p. JW4A.83, 2012.

[30] L. Chen, C. R. Doerr, and Y.-K. Chen, "Compact polarization rotator on silicon for polarization-diversified circuits," *Optics Letters*, vol. 36, p. 469, Feb. 2011.

[31] J. D. Sarmiento-Merenguel, R. Halir, X. Le Roux, C. Alonso-Ramos, L. Vivien, P. Cheben, E. Durán-Valdeiglesias, I. Molina-Fernández, D. Marris-Morini, D.-X. Xu, J. H. Schmid, S. Janz, and A. Ortega-Moñux, "Demonstration of integrated polarization control with a 40 dB range in extinction ratio," *Optica*, vol. 2, p. 1019, Dec. 2015.

[32] M. Ibrahim, J. H. Schmid, A. Aleali, P. Cheben, J. Lapointe, S. Janz, P. J. Bock, A. Densmore, B. Lamontagne, R. Ma, D.-X. Xu, and W. N. Ye, "Athermal silicon waveguides with bridged subwavelength gratings for TE and TM polarizations," *Optics Express*, vol. 20, p. 18356, July 2012.

[33] Q. Xu, L. Chen, M. G. Wood, P. Sun, and R. M. Reano, "Electrically tunable optical polarization rotation on a silicon chip using Berry's phase," *Nature Communications*, vol. 5, p. 5337, Nov. 2014.

[34] G. Reed and A. Knights, *Silicon Photonics: An Introduction*. Wiley, 2004.

[35] "Wave–particle duality." `https://en.wikipedia.org/wiki/Wave%E2%80%93particle_duality`, Jan. 2016. [Online; accessed 07-Feb-2016].

[36] "Maxwell's equations." https://en.wikipedia.org/w/index.php?title=Maxwell%27s_equations&oldid=702587090, Jan. 2016. [Online; accessed 07-Feb-2016].

[37] G. T. Reed, *Silicon Photonics: The State of the Art*. New York, NY, USA: Wiley-Interscience, 2008.

[38] J. M. Burch and A. Gerald, *Introduction to Matrix Methods in Optics*. John Wiley & Sons, 1st ed., 1975.

[39] F. Flossmann, U. T. Schwarz, M. Maier, and M. R. Dennis, "Stokes parameters in the unfolding of an optical vortex through a birefringent crystal," *Optics Express*, vol. 14, no. 23, p. 11402, 2006.

[40] H.-T. Wang, X.-L. Wang, Y. Li, J. Chen, C.-S. Guo, and J. Ding, "A new type of vector fields with hybrid states of polarization," *Optics Express*, vol. 18, p. 10786, May 2010.

[41] "Optical polarization waves." http://www.wikiwand.com/en/Polarization_(waves), 2015. [Online; accessed 09-Feb-2016].